Science Advances
AAAS

advances.sciencemag.org/cgi/content/full/sciadv.aba7910/DC1

Supplementary Materials for

Viruses harness YxxØ motif to interact with host AP2M1 for replication: a vulnerable broad-spectrum antiviral target

Shuofeng Yuan, Hin Chu, Jingjing Huang, Xiaoyu Zhao, Zi-Wei Ye, Pok-Man Lai, Lei Wen, Jian-Piao Cai, Yufei Mo, Jianli Cao, Ronghui Liang, Vincent Kwok-Man Poon, Kong-Hung Sze, Jie Zhou, Kelvin Kai-Wang To, Zhiwei Chen, Honglin Chen, Dong-Yan Jin, Jasper Fuk-Woo Chan,* Kwok-Yung Yuen*

*Corresponding author. Email: kyyuen@hku.hk (K.-Y.Y.); jfwchan@hku.hk (J.F.-W. C.)

Published 14 August 2020, *Sci. Adv.* **6**, eaba7910 (2020)
DOI: 10.1126/sciadv.aba7910

This PDF file includes:

Other Supplementary Material for this manuscript includes the following:

(available at advances.sciencemag.org/cgi/content/full/sciadv.aba7910/DC1)

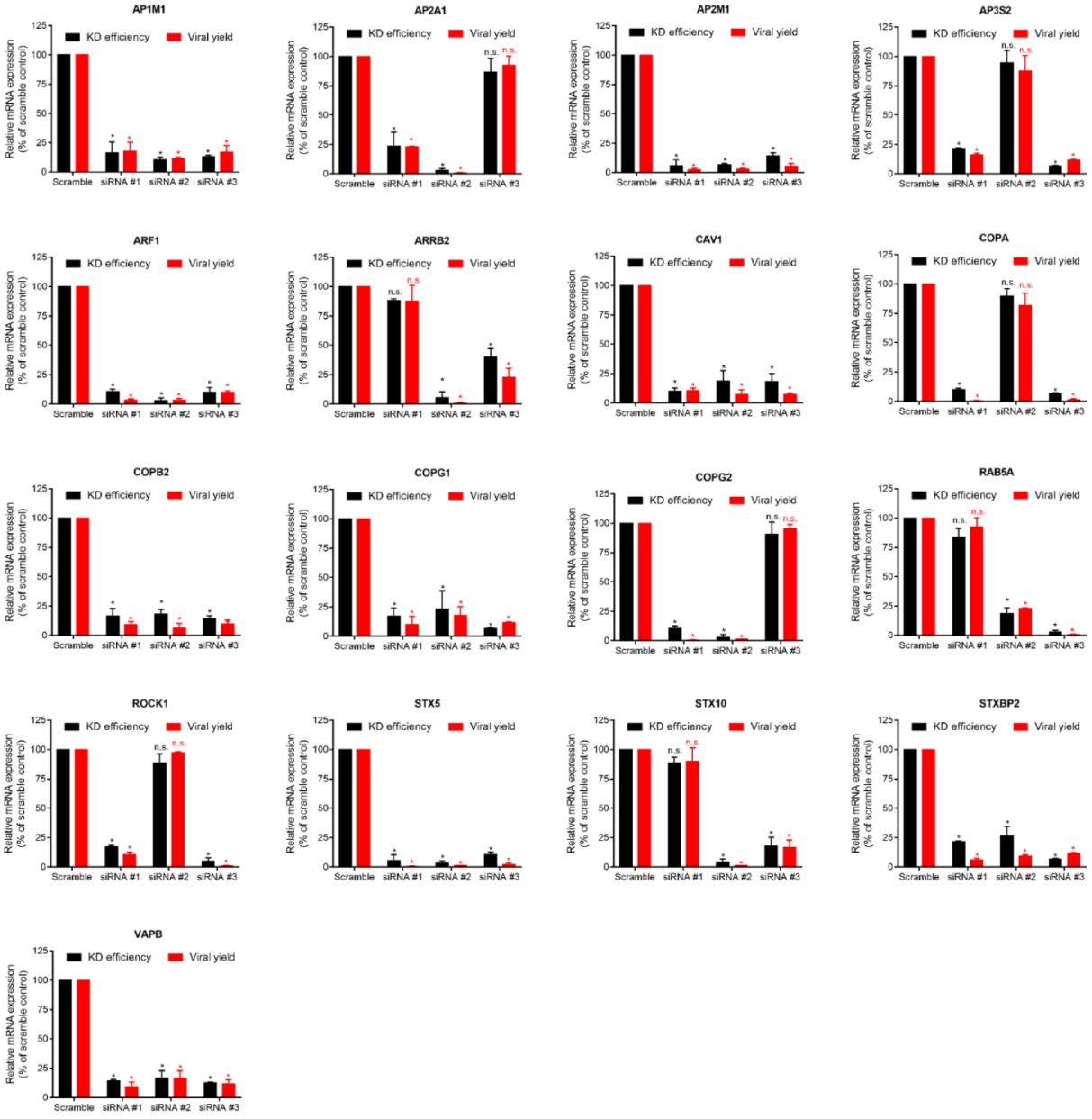

Fig. S1. Validation of the pro-viral activity of the selected host genes (corresponding to Fig.1B). Three unique, non-overlapping siRNAs targeting each of 17 selected genes was transfected into A549 cells for 48h, followed by H1N1 infection (0.1 MOI) for another 48h. Transcript level (black bars) of the host genes after siRNA knock down and corresponding viral load (red bars) were determined by RT-qPCR assays. Differences between groups were compared with the scramble control groups using one-way ANOVA. Shown are the mean value ± s.d. of triplicate samples. *$p<0.05$, n.s. indicates $p>0.05$.

A

Virus family	Virus (strain)	Cell line	EC_{50} (μM)	CC_{50} (μM)	SI (CC_{50}/EC_{50})
Orthomyxoviridae	Influenza A(H1N1)pdm09	MDCK	0.42±0.09	92±4	219.0
Retroviridae	HIV-1(JR-FL)	MOLT4	7.89±2.64	116±5	14.7
Flaviviridae	ZIKV (PRVABC59)	Vero	2.42±0.21	29±2	12.0
Coronaviridae	SARS-CoV-2 (HKU-001a)	Caco2	0.59±0.21	89±4	150.8
	MERS-CoV (HCoV-EMC/2012)	Huh7	2.50±0.25	23±3	9.2
	SARS-CoV (GZ50)	Vero	1.12±0.14	29±2	25.9
Picornaviridae	EV-A71 (SZ/HK05)	RD	1.35±0.25	45±5	33.3
	HRV-B14 (1059)	RD	5.38±0.51	45±5	8.4
Phenuiviridae	SFTSV (HB29)	Huh7	0.59±0.04	23±3	39.0
Adenoviridae	AdV5 (clinical isolate)	HEp-2	1.25±0.09	39±4	31.2

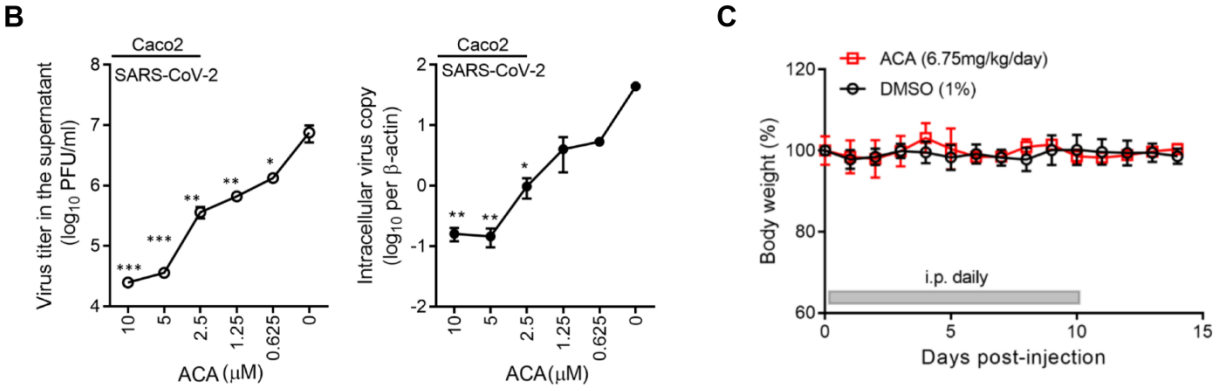

Fig. S2. Antiviral activity and cytotoxicity of ACA (corresponding to Fig.1C and Fig.2G). (A) EC_{50} of ACA against different families of viruses were plotted by plaque reduction assay (pdmH1N1, ZIKV, SARS-CoV-2, MERS-CoV, SARS-CoV, EV-A71, HRV-B14) or $TCID_{50}$ (SFTSV, AdV5) or p24 antigen ELISA (HIV-1), whereas CC_{50} of ACA in different cell lines were determined by measuring the cellular NAD(P)H-dependent cellular oxidoreductase enzymes (MTT assay). Selectivity index (SI) is calculated by the ratio from CC_{50} to EC_{50}. (B) Caco2 cells were infected with SARS-CoV-2 (0.1 MOI) and treated with different concentrations of ACA as indicated. Infectious virus titer in the cell culture supernatant were collected at 48hpi and determined by standard plaque assay. Intracellular viral loads were quantified by qRT-PCR targeting the SARS-CoV-2 RdRp/Helicase region and were normalized by human β-actin. One-way ANOVA was used to compare the treatment groups with the 0μM (negative control) group. *P indicates < 0.05 and ** indicates P < 0.01 (One-way ANOVA). The experiments were performed in triplicate and replicated twice. The results are shown as mean ± standard deviations. (C) *In vivo* toxicity of ACA to BALB/c mice (n=5, 8-10 weeks) were checked by intraperitoneal (i.p.) injection of ACA or DMSO (1%) for 10 days. Shown is the body weight change of each group recorded for 14 days. The result is shown as mean body weight each day ±s.d.

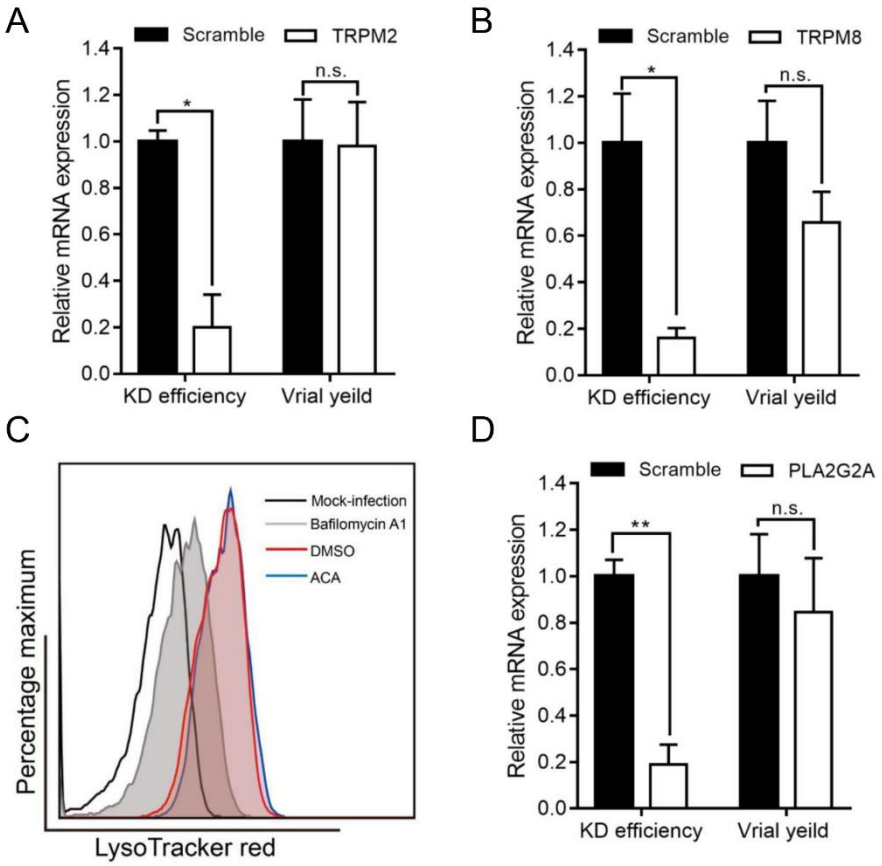

Fig. S3. Antiviral activity of ACA was not dependent on the blockage of TRP channel nor the inhibition of phospholipase A2 (corresponding to Fig. 4A**)**. (A and B) A549 cells were transfected with TRPM2-targeted siRNA (A) or TRPM8-targeted siRNA (B) for 48h, followed by H1N1 infection (0.1 MOI) for another 48h. Efficiency of siRNA knock-down was detected before virus infection by RT-qPCR. Viral load in the cell culture supernatants was quantified by detecting the viral M-gene copies. Differences between groups were compared by Student's t-test. *$p<0.05$, n.s. indicates $p>0.05$. (C) To determine whether the acidity of the endosomal/lysosomal compartments was changed by ACA due to its ion channel blockage activity, MDCK cells were infected by 10MOI pdmH1N1 virus for 75 min at 4◦C, followed by ACA (20μM) or DMSO (0.1%) or Bafilomycin A1 (100nM) for 1h at 37 °C. After that, cells were stained with 50 nM LysoTracker red (LTR) before its fluorescence intensity was measured by flow cytometry. Shown is the one of three independent assays with similar results. (D) Virus replication after host PLA2G2A gene knockdown was determined using the same protocol as described in (A) and (B). **$p<0.01$. The experiments were performed in triplicate and in 3 independent experiments. Data in bar charts are presented as mean values ±standard deviation.

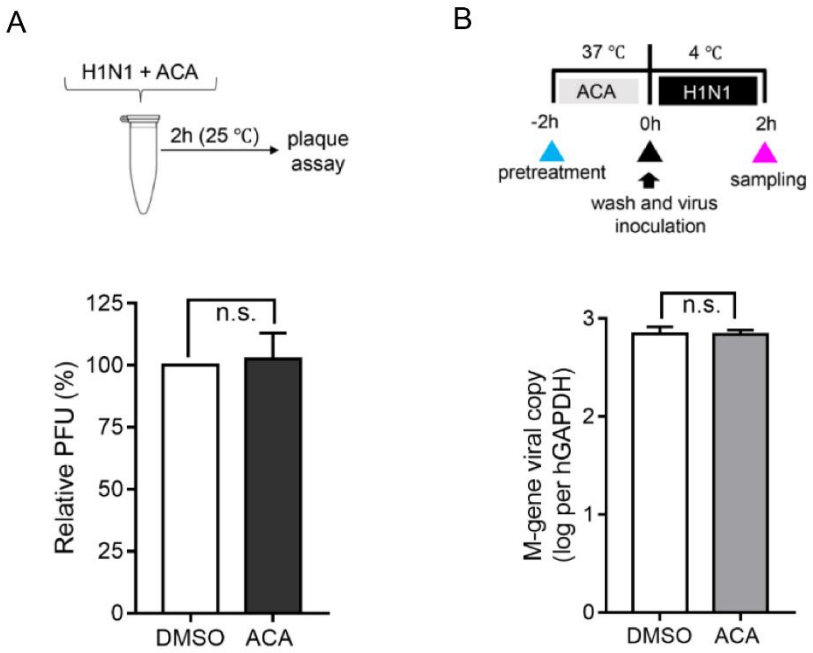

Fig. S4. ACA did not inactivate viral particles nor inhibit virus attachment (corresponding to Fig. 4A). To explore the stages of viral life cycle that ACA interfered with, (A) virus inactivation assay: pdmH1N1 virus (10^6 PFU) was incubated with ACA(20μM) for 2 h, followed by standard plaque assay from diluting the mixture for 10,000 fold (i.e. the remaining concentration of ACA was below its EC_{50} thus did not affect the plaque formation). Shown is the relative PFU when compared with the DMSO control (0.1%). (B) virus attachment assay: MDCK cells were pre-treated by ACA(20μM) for 2 h, followed by intensive wash and shifted to 4 ℃ incubation with virus (MOI=5). After 2 h, the virus inoculum was removed, cells were washed twice before lysis, and the attached viral RNA load was determined by qRT-PCR. The experiments were carried out in triplicate. Data are presented as mean values ±standard deviations and analyzed by Student's t-test, n.s. indicates $p>0.05$.

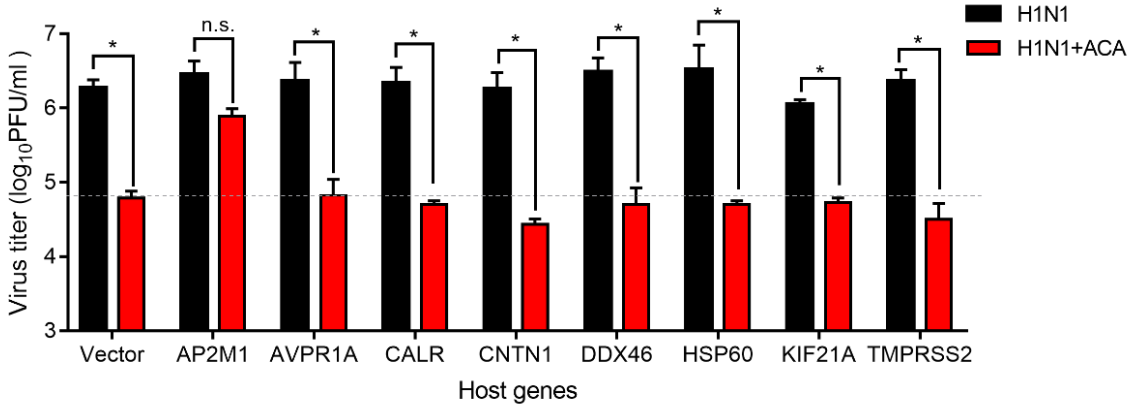

Fig. S5. Functional validation assay of ORF clones as revealed by the protein ID analyses. (corresponding to Fig. 4D). Individual plasmid (500ng) were transfected to MDCK for 24h before pdmH1N1 virus infection (0.001MOI) and ACA (5μM) treatment. Virus titer in the supernatant was collected at 24hpi and determined by plaque assay. Student's t-test was performed to evaluate each gene's capacity to rescue pdmH1N1 virus replication against ACA. *$p<0.05$, n.s. indicates $p>0.05$ when compared with non-ACA-treated group. The experiments were carried out in triplicate and in 3 independent experiments.

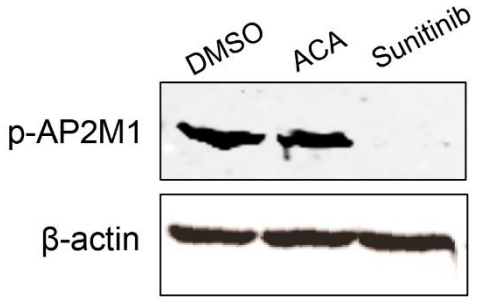

Fig. S6. ACA did not inhibit AP2M1 phosphorylation (corresponding to Fig. 5A). The effect of the inhibitors on AP2M1 phosphorylation by Western blotting analysis of HBTEC cell lysates harvested following 10MOI pdmH1N1 infection and treatment with the compounds in the presence of Calyculin A (Cal-A). Representative membranes blotted with anti-phopho-AP2M1 (p-AP2M1) and anti-β-actin antibodies.

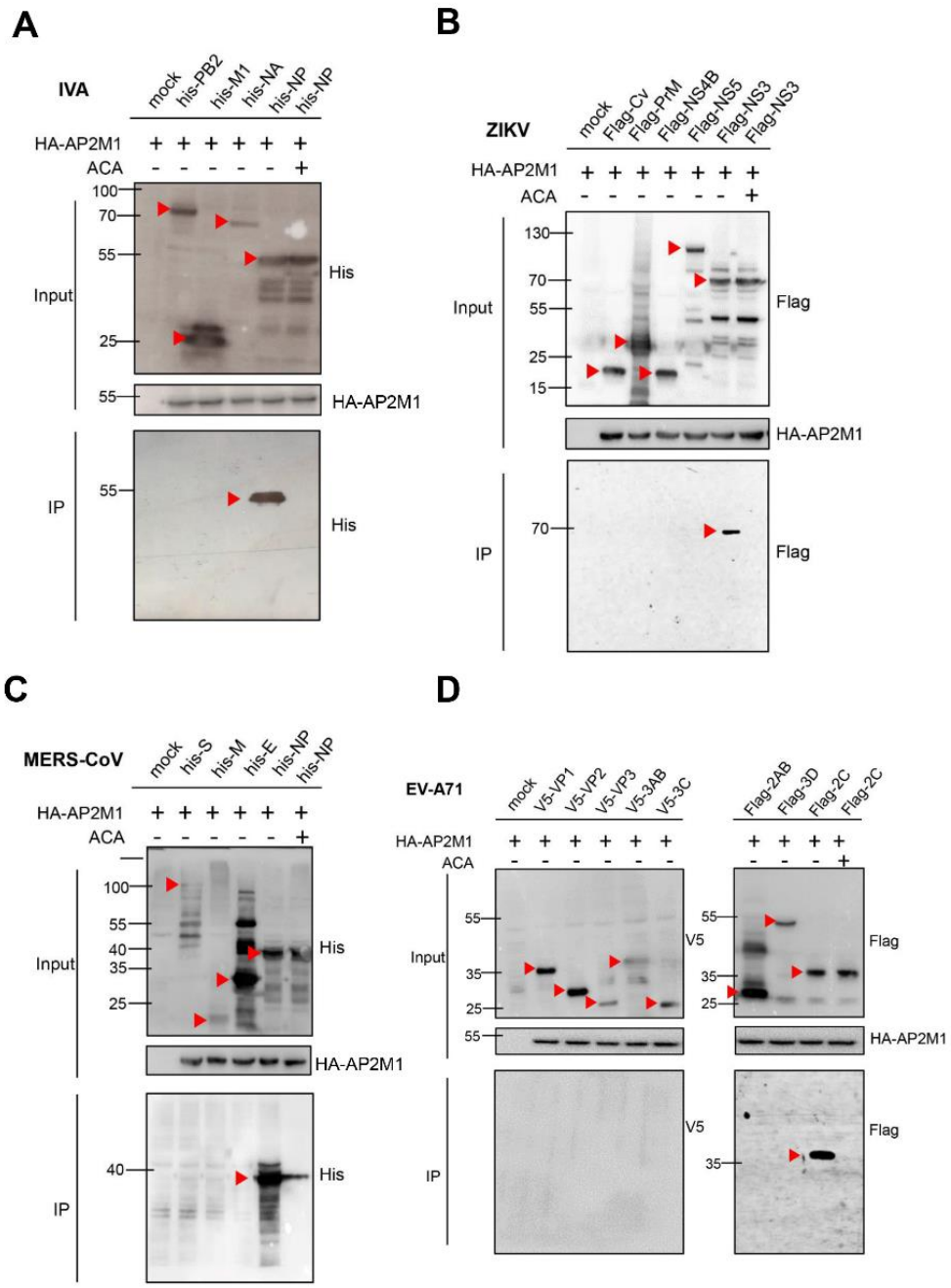

Fig. S7. AP2M1 interacts with different viral proteins (corresponding to Fig. 5A and Fig. 5G). Immunoprecipitations (IPs) of AP2M1 and individual viral protein identified influenza A virus NP (A), ZIKV NS3 (B), MERS-CoV NP (C) and EV-A71 2C (D) as their respective and specific binding partners. Candidate viral proteins in each virus panel were co-transfected with HA-tagged AP2M1 in HEK293T cells and in the presence or absence of ACA (10μM) as indicated. IPs were performed using the anti-HA magnetic beads. All the input AP2M1 were detected by AP2M1-specific antibodies while individual viral protein by anti-flag or anti-V5 or anti-His as indicated. Red triangle indicates the target protein band.

Position 296-299	Y	X	X	Ø
WT	Y	S	L	V
Y296A	A	S	L	V
Ø299A	Y	S	L	A
Ø299L	Y	S	L	L
Position 385-388	**Y**	**X**	**X**	**Ø**
WT	Y	W	A	I
Y385A	A	W	A	I
Ø388A	Y	W	A	A
Ø388L	Y	W	A	L

Fig. S8. The sequences of all engineered NP mutants used in this study (corresponding to Fig. 6A and Fig. 6C). Two YxxØ motif are identified in influenza A NP protein, Y is tyrosine, x is any amino acid, and Ø is an amino acid with a bulky hydrophobic side chain referring to L/M/F/I/V. Substitution in each mutant is highlighted in red.

Table S1 Anti-influenza effective compounds identified from the library screening

Name	Target(s)
With 2-logs viral load reduction at 1μM[a]	
ACA	TRP Channel; PLA2
Pyr6	TRP Channel
Imperatorin	AChE; TRP Channel
Ethosuximide	Calcium Channel
ZD7288	HCN Channel
With 3-logs viral load reduction at 10μM[a]	
Cariporide	Sodium Channel
Dyclonine (hydrochloride)	Sodium Channel
Anabasine	nAChR
GTS-21 (dihydrochloride)	nAChR
Adiphenine (hydrochloride)	nAChR
Fanapanel	iGluR
PEAQX (tetrasodium hydrate)	iGluR
(-)-Dizocilpine (Maleate)	iGluR
Lorediplon	GABA Receptor
Riluzole hydrochloride	GABA Receptor; Sodium Channel
Oxiracetam	GABA Receptor
Gliclazide	Potassium Channel
4-Aminopyridine	Potassium Channel
Nilvadipine	Calcium Channel
Rosiglitazone	Autophagy; PPAR; TRP Channel
SB-366791	TRP Channel
CGP37157	Na+/Ca2+ Exchanger
Prilocaine	Na+/K+ ATPase
p-Hydroxybenzaldehyde	Endogenous Metabolite; GABA Receptor
UK-5099	Monocarboxylate Transporter

[a] as detected by RT-qPCR targeting M-gene of Influenza A virus.

Table S2 Primers used in this study

Name	Sequence (5' to 3')
Primers for mutagenesis study	
AP2M1_M216A_F	GAATGCAAGTTTGGGGCGAATGACAAGATTGT
AP2M1_M216A_R	ACAATCTTGTCATTCGCCCCAAACTTGCATTC
AP2M1_N217A_F	ATGCAAGTTTGGGATGGCTGACAAGATTGTTAT
AP2M1_N217A_R	ATAACAATCTTGTCAGCCATCCCAAACTTGCAT
AP2M1_K400A_F	ATTCGCGCCCTCTGGCCTCGCAGTGCGCTACTTGAAGGT
AP2M1_K400A _R	ACCTTCAAGTAGCGCACTGCGAGGCCAGAGGGCGCGAAT
AP2M1_K410A_F	GAAGGTGTTTGAACCGGCGCTGAACTACAGCGACC
AP2M1_K410A _R	GGTCGCTGTAGTTCAGCGCCGGTTCAAACACCTTC
AP2M1_ D176A_F	GTCGGAATGAGCTCTTCCTGGCTGTGCTGGAGAGTGTGAACC
AP2M1_D176A _R	GGTTCACACTCTCCAGCACAGCCAGGAAGAGCTCATTCCGAC
Influenza A_NP_Y296A_F	CTTCGAGAGAGAAGGAGCCTCTCTGGTTGGGATAG
Influenza A_NP_Y296A_R	CTATCCCAACCAGAGAGGCTCCTTCTCTCTCGAAG
Influenza A_NP_Ø299A_F	GAGAAGGATACTCTCTGGCTGGGATAGATCCTTTCCG
Influenza A_NP_ Ø299A_R	CGGAAAGGATCTATCCCAGCCAGAGAGTATCCTTCTC
Influenza A_NP_Ø299L_F	GAGAAGGATACTCTCTGCTTGGGATAGATCCTTTCCG
Influenza A_NP_ Ø299L _R	CGGAAAGGATCTATCCCAAGCAGAGAGTATCCTTCTC
Influenza A_NP_Y385A_F	ACTTGAGCTGAGAAGTAGAGCTTGGGCTATAAGAACCAGGAG
Influenza A_NP_Y385A _R	CTCCTGGTTCTTATAGCCCAAGCTCTACTTCTCAGCTCAAGT
Influenza A_NP_Ø388A_F	GAAGTAGATATTGGGCTGCAAGAACCAGGAGCGGAGG
Influenza A_NP_ Ø388A _R	CCTCCGCTCCTGGTTCTTGCAGCCCAATATCTACTTC
Influenza A_NP_Ø388L_F	GAAGTAGATATTGGGCTCTAAGAACCAGGAGCGGAGG
Influenza A_NP_ Ø388L _R	CCTCCGCTCCTGGTTCTTAGAGCCCAATATCTACTTC
Primers for differentiate the viral vRNA, cRNA and mRNA	
Influenza A_NP_ vRNA_F	GGCCGTCATGGTGGCGAAT GAATGGACGGAGAACAAGGATTGC
Influenza A_NP_ vRNA_R	CTCAATATGAGTGCAGACCGTGCT
Influenza A_NP_ vRNA_tag	GGCCGTCATGGTGGCGAAT
Influenza A_NP_ cRNA_F	CGATCGTGCCCTCCTTTG
Influenza A_NP_ cRNA_R	GCTAGCTTCAGCTAGGCATC AGTAGAAACAAGGGTATTTTTCTTT
Influenza A_NP_ cRNA_tag	GCTAGCTTCAGCTAGGCATC
Influenza A_NP_ mRNA_F	CGATCGTGCCCTCCTTTG
Influenza A_NP_ mRNA_R	CCAGATCGTTCGAGTCGT TTTTTTTTTTTTTTTTCTTTAATTGTC
Influenza A_NP_ mRNA_tag	CCAGATCGTTCGAGTCGT
Primers for qPCR detection of viral and host genes	
Influenza A_M_F	CTTCTAACCGAGGTCGAAACG
Influenza A_M_R	GGCATTTTGGACAAAKCGTCTA
PLA2G2A_F	AAGGAAGCCGCACTCAGTTA
PLA2G2A_R	TTGCACAGGTGATTCTGCTC
TRPM2_F	GGCAGCCTTGTACTTCAGTGAC
TRPM2_R	GAGGCAGAACAGGATGAAGTCC
TRPM8_F	CTGGTTGCGAACTTCCGAAGAG
TRPM8_R	GGTGCCGAGTAATAGGAGACAC
human GAPDH_F	ATTCCACCCATGGCAAATTC

human GAPDH_R	CGCTCCTGGAAGATGGTGAT
mouse GAPDH_F	AAGGTCATCCCAGAGCTGAA
mouse GAPDH_R	CTGCTTCACCACCTTCTTGA

Supplementary movies

Movie S1 (corresponding to Fig. 5F). Co-trafficking of influenza A GFP labelled NP (Green) with mCherry fused AP2M1 (Red) upon DMSO vehicle treatment. Representative video of time-lapse images were taken in a heated (37°C) chamber. Individual co-localized puncta run lengths and transport velocities were calculated using the Track Points for MetaMorph analysis software.

Movie S2 (corresponding to Fig. 5F). Co-trafficking of influenza A NP (Green) with AP2M1 (Red) upon ACA treatment. Representative video taken as specified in Video 1.